An *E. coli*-produced Single-chain Variable Fragment (scFv) Targeting Hepatitis B Virus Surface Protein Potently Inhibited Virion Secretion

Cheng Li[a†], Yang Wang[a†], Tiantian Liu[a], Matthias Niklasch[c], Ke Qiao[a], Sarah Durand[d], Li Chen[a], Mifang Liang[b], Thomas F. Baumert[d,e,f], Shuping Tong[a], Michael Nassal[c], Yu-Mei Wen[a], Yong-Xiang Wang[a*]

[a]Key Laboratory of Medical Molecular Virology, Ministry of Education and Ministry of Health, Shanghai Medical College of Fudan University, Shanghai, China

[b]Key Laboratory for Medical Virology, NHFPC, National Institute for Viral Disease Control and Prevention, China CDC, Beijing, China

[c]University Hospital Freiburg, Department of Internal Medicine II/Molecular Biology, Freiburg, Germany

[d]Inserm, U1110, Institut de Recherche sur les Maladies Virales et Hépatiques, Strasbourg, France

[e]Université de Strasbourg, Strasbourg, France

[f]Institut Hospitalo-Universitaire, Pôle 5 Hépato-digestif, Nouvel Hôpital Civil, Strasbourg, France

Running title: Anti-HBs scFv blocking HBV infection and virion secretion

[†]These authors contributed equally to this work.

*Corresponding author, Key Laboratory of Medical Molecular Virology, Ministry of Education and Ministry of Health, Shanghai Medical College of Fudan University, 200032 Shanghai, China.

Email: yongxiangwang@fudan.edu.cn

Abbreviations: scFv, single-chain variable fragment; HBV, hepatitis B virus; S, small surface protein; M, middle surface protein; L, large surface protein; HBsAg, hepatitis B surface antigen; AGL, antigenic loop; HBIG, hepatitis B immune globulin; IC_{50}, 50% inhibitory concentration; mAb, monoclonal antibody; IFN-α, interferon α; NA, nucleos(t)ide analogue; SVP, subviral particle; NTCP, sodium-taurocholate cotransporting polypeptide; MVB, multivesicular body; Ig, immunoglobulin; VL, variable region of light chain; VH, variable region of heavy chain; IMAC, immobilized metal ion affinity chromatography; LCM, laser confocal microscopy; PHH, primary human hepatocyte; NAGE, native agarose gel electrophoresis; ELISA, enzyme linked immunosorbent assay.

Abstract

Hepatitis B virus (HBV) envelopes as well as empty subviral particles carry in their lipid membranes the small (S), middle (M), and large (L) surface proteins, collectively known as hepatitis B surface antigen (HBsAg). Due to their common S domain all three proteins share a surface-exposed hydrophilic antigenic loop (AGL) with a complex disulfide bridge-dependent structure. The AGL is critical for HBV infectivity and virion secretion, and thus represents a major target for neutralizing antibodies. Previously, a human monoclonal antibody (mAb) targeting a conformational epitope in the AGL, IgG12, exhibited 1,000-fold higher neutralizing activity than hepatitis B immune globulin (HBIG). Here we designed a single-chain variable fragment (scFv) homolog of IgG12, G12-scFv, which could be efficiently produced in soluble form in the cytoplasm of *E. coli* SHuffle cells. Independent in vitro assays verified specific binding of G12-scFv to a conformational S epitope shared with IgG12. Despite 20-fold lower affinity, G12-scFv but not an irrelevant scFv potently neutralized HBV infection of susceptible hepatoma cells (IC_{50}=1.8 nM). Strikingly, low concentrations of G12-scFv blocked virion secretion from HBV producing cells (IC_{50}=1.25 nM) without disturbing intracellular viral replication, whereas extracellular HBsAg was reduced only at >100-fold higher though still nontoxic concentration. The inhibitory effects correlated with S binding specificity and presumably also G12-scFv internalization into cells. Together these data suggest G12-scFv as a highly specific yet easily accessible novel tool for basic, diagnostic, and possibly future therapeutic applications.

1. Introduction

Current therapies for chronic hepatitis B (CHB), i.e. free or pegylated interferon α (IFN-α) and nucleos(t)ide analogues (NAs) (Trepo et al., 2014), only rarely achieve loss of HBsAg in the treated patients (3-7% for IFN-α; ~1% per year for NAs) and suffer from adverse effects and unpredictable duration of treatment (Zeisel et al., 2015). Hence there is an urgent need for the development of new anti-HBV therapeutics, including antibodies (Salazar et al., 2017).

Sera of HBV infected patients contain complete genome-containing virions, genome-free empty virions (Hu and Liu, 2017) plus a huge excess (up to 10^5-fold) of empty envelopes termed subviral particles (SVPs). All these particles contain membrane embedded S, M, and L surface proteins, although the L protein content is highest in virions (Heermann et al., 1984). M and L are extended versions of S carrying an extra 55 amino acid (aa) PreS2 (M) or extra PreS1 (108, 118, or 119 aa) plus PreS2 region (L) on their N termini. The 226-aa S protein is the most abundant among the surface proteins. Between the second and third of its four proposed transmembrane domains and comprising approximately aa 99-169 lies the AGL. It is exposed on the surface of virions and SVPs, and presents the dominant linear and conformational epitopes for neutralizing antibodies (Zanetti et al., 2008). Within the AGL, aa from about position 120-150 form the highly conformational epitopes of the “a” determinant which is rich in disulfide-bond forming cysteine residues (Mangold et al., 1995; Wounderlich and Bruss, 1996). Furthermore, this region interacts with heparan sulfate proteoglycans, concentrating virions on the cell surface for

subsequent high affinity interactions between PreS1 part of L protein and the HBV receptor sodium-taurocholate cotransporting polypeptide (NTCP) (Sureau and Salisse, 2013; Verrier et al., 2016); hence beyond PreS1 the AGL is a pivotal viral determinant of HBV infectivity. Accordingly, many mutations and/or disruption of the disulfide-bond network in the AGL interfere with viral infectivity (Urban et al., 2014), and antibodies targeting the AGL, like those targeting PreS1 such as mAb MA18/7 (Glebe et al., 2003), can possess virus neutralizing activity (Urban et al., 2014), the basis of prophylactic vaccination with S protein.

Egress of HB virions and SVPs remain mechanistically elusive but are believed to proceed through different routes. SVP assembly likely initiates in the post-endoplasmic reticulum/pre-Golgi compartment, with particle secretion via the general secretory pathway (Huovila et al., 1992; Patzer et al., 1984). Mature nucleocapsids filled with relaxed circular DNA (rcDNA), and likely also empty capsids (Ning et al., 2017), are enveloped by interacting with the PreS parts of L on the cytosolic side of the ER membrane (Hu and Liu, 2017; Kluge et al., 2005; Pairan and Bruss, 2009), followed by budding into the multivesicular body (MVB) compartment of late endosomes (Kian Chua et al., 2006; Lambert et al., 2007; Watanabe et al., 2007) and finally exiting the cell via an exosomal pathway (Watanabe et al., 2007). Notably, the AGL is also pivotal for secretion of virions and SVPs as shown by the impaired secretion of naturally occurring AGL mutants (Chen et al., 2016; Khan et al., 2004; Kwei et al., 2013). Furthermore, high concentrations (≥100 μg/ml) of exogenously added AGL-specific immunoglobulins (Igs)

reportedly allowed internalization and interference with secretion of viral particles, although the exact particle types were not clearly discriminated (Neumann et al., 2010; Schilling et al., 2003).

Recently, we developed a human anti-HBs mAb IgG12 with very high affinity (Kd=7.56 nM). IgG12 recognizes a conformational epitope in the AGL, most likely the "a" determinant, and displayed >1,000-fold higher HBV neutralizing activity than HBIG (Wang et al., 2016). Moreover, a one-dose administration of IgG12 into HBV transgenic mice achieved a prolonged (144-day) suppression of serum HBsAg levels (Wang et al., 2016). This might be due to immune-modulatory functions of IgG, e.g. Fc-Fcγ receptor mediated effects, yet also to the potential blockade of virion secretion by internalized IgG (Neumann et al., 2010; Zhang et al., 2016). However, the large size of ~150 KDa of a complete mAb probably limits its tissue penetration ability and, furthermore, mAb production is still very costly (Elgundi et al., 2017; Li et al., 2016).

Meanwhile, various antibody derivatives with simpler architectures such as antigen binding fragment (Fab), variable fragment (Fv), or single chain variable fragment (scFv) have been engineered, often using a well-characterized parental mAb as template. In scFvs, the variable regions of the light chain (VL) and of the heavy chain (VH) are covalently joined by a flexible peptide linker, e.g. $([G]_4S)_3$. Ideally, the resulting single ~30 kDa polypeptide combines the binding specificity of the parental mAb with improved tissue penetration, lower immunogenicity and potentially less demanding and

less costly host requirements for production (Li et al., 2016; Saeed et al., 2017). This also facilitates further application-specific engineering, e.g. by linking the scFv to dyes, radionuclides, drugs, or other protein moieties. However, the simple monovalent scFv design also reduces avidity and possibly specificity and affinity for the target, with potentially strong negative impacts on neutralization potency which, in addition, may be influenced by the absence vs. presence of the Fc part (Chan et al., 2015; Kang et al., 2018; Sela-Culang et al., 2013; Torres and Casadevall, 2008).

Here we aimed to exploit scFv technology to generate an *E. coli* expressable derivative of mAb IgG12, termed G12-scFv. As shown below G12-scFv could be solubly expressed in the cytoplasm of *E. coli* SHuffle cells and purified in amounts of ~2 mg/liter bacterial culture by immobilized metal ion affinity chromatography (IMAC). In vitro interaction assays, including competition with IgG12, confirmed specific, high affinity binding of G12-scFv to HBsAg and potent HBV neutralizing activity in cell culture infection experiments. Strikingly, very low concentrations of G12-scFv selectively inhibited virion release from stably HBV producing cells whereas higher concentrations were required for clear reductions in SVP secretion. Tracking native and fluorescently labeled G12-scFv by laser confocal microscopy (LCM) as well as endocytosis inhibition using specific inhibitors supported a model whereby the anti-virion effect correlates with G12-scFv internalization such that it preferentially encounters virions rather than SVPs. Hence G12-scFv and/or further optimized derivatives such as G12 diabodies should represent highly specific yet easily accessible tools for HBV-related basic studies as well as

diagnostic and possibly therapeutic applications.

2. Materials and methods

2.1 Plasmid constructs

The *E. coli* expression vectors pET28a-His-G12-scFv-HA, pET28a-His-MA18/7-scFv-HA and pET28a-His-VRC01-scFv-HA, encode between Nde I and Xho I restriction sites the VL and VH domains of mAbs G12 and MA18/7 against HBV S and PreS1 (Kuttner et al., 1999; Wang et al., 2016), and of VRC01, targeting gp120 of human immunodeficiency virus 1 (HIV-1) (Wu et al., 2010), fused by the flexible linker $([G]_4S)_3$ plus C-terminal HA tags. pET28a-His-G12-scFv-HCdel-HA encodes a mutated G12-scFv with deletion of 11 amino acids of the complementarity determining region 3 (CDR3) of VH. pCDNA6-NTCP-C9 harbors a codon-optimized open reading frame (ORF) for NTCP (GenBank accession no. NM_003049) with a C terminal C9 tag. pCH-9/3091 comprises a 1.05-fold HBV genome (genotype D, GenBank accession no. V01460) in which pre-genomic RNA (pgRNA) transcription is controlled by the cytomegalovirus immediate early (CMV-IE) promoter (Nassal, 1992).

2.2 Cell culture, HBV infection, and plasmid transfection

Huh-7 and HepG2 hepatoma cells, HepG2.2.15 (abbreviated as 2.2.15 hereafter) and HepAD38 were cultured as previously described (Ladner et al., 1997; Sells et al., 1987). Primary human hepatocytes (PHHs) were isolated from liver resection tissue and cultured as described previously (Krieger et al., 2010; Mailly et al., 2015). The

respective protocols for the use of human materials were approved by the Ethics Committee of the University of Strasbourg Hospitals (CPP 10-17). A HepG2 cell line stably expressing C9-tagged NTCP was established by transfection with Sal I-linearized pCDNA6-NTCP-C9 and subsequent selection with 5 μg/ml blasticidin. HBV infection of HepG2-NTCP cells was performed as previously reported (Ni et al., 2014). Transfections were performed using TransIT-LT1 reagent (Mirus) as recommended by the manufacturer.

2.3 Protein expression and purification

Bacterial expression using *E. coli* SHuffle-T7 (New England Biolabs) or BL21 (DE3) Star (ThermoFisher Scientific) as the hosts and subsequent purification of the scFvs for G12, MA18/7, and VRC01 were performed using previously reported methods (Wang et al., 2012). Briefly, *E. coli* hosts transformed with scFv expressing vectors were cultured in Luria-Bertani broth containing 0.5 mM isopropyl β-D-thiogalactoside (IPTG) at 30°C overnight to induce scFv expression. Bacteria were homogenized by ultrasonic treatment in the lysis buffer (20 mM Tris-HCl pH 7.5, 150 mM NaCl, 0.5% Triton X-100; 10 mM $MgCl_2$, 1 mg/ml lysozyme, 50 μg/ml RNase A, 5 μg/ml DNase I, and protease inhibitor cocktails [Roche]). After centrifugation at 12,000 g for 30 min at 4°C, soluble scFvs in the clear supernatants were purified by IMAC with a Ni-nitrilotriacetic acid (Ni-NTA) Superflow column (Qiagen). Finally, the scFvs were dialyzed against PBS and concentrated by Amicon centrifugal filtration devices (Millipore) with a molecular cutoff of 3 KDa.

2.4 Native agarose gel electrophoresis (NAGE) of viral particles

PEG precipitated HBV particles from culture supernatants were separated into virions and naked capsids by NAGE in 1% agarose gels run in 1×TAE buffer and transferred onto nylon membranes (Wang et al., 2012). Virion-derived capsid and naked capsid were probed by sequential incubation with polyclonal rabbit anti-core serum, peroxidase-conjugated anti-rabbit secondary antibody, and ECL reagents (PerkinElmer).

2.5 Extraction of cytoplasmic capsid-borne viral DNAs and nuclear DNAs, Western blotting and Southern Blotting

Details are given in the supplementary materials & methods.

2.6 Extraction of virion DNAs and qPCR

Details are also given in the supplementary materials & methods.

2.7 Enzyme linked immunosorbent assay (ELISA)

Microwell plates coated respectively with 5 μg/ml G12-scFv, VRC01-scFv, or IgG12 were incubated with various concentrations of Chinese hamster ovary (CHO) cell-expressed S protein or sera from healthy donors or CHB patients, diluted 1:10 in PBS, at 37°C for 1 h, and subsequently reacted with peroxidase-conjugated anti-S (Shanghai Kehua Bio-Engineering Company, KHB). After extensive washing, the plates

were developed using 3, 3', 5, 5'-tetramethylbenzidine (KHB) as substrate with subsequent stopping by sulphuric acid. Absorbance values at 450 nm ($A_{450\ nm}$) were recorded by an ELISA plate reader (Biorad). HBe and HBs antigens in culture supernatants were measured using commercial ELISA kits (KHB) according to the manufacturer's manuals. For the competitive G12-scFv vs. IgG12 ELISA microwell plates coated with recombinant S protein (KHB) were incubated with 50 ng/ml IgG12 plus increasing concentrations (ranging from 10 ng/ml to 20,000 ng/ml) of G12-scFv per well. After incubation and washing, the plates were reacted with a peroxidase-conjugated antibody targeting the Fc region of human IgG (a gift from Tianlei Ying, Fudan University) and processed as described above.

2.8 Biolayer interferometry

Biolayer interferometry (Concepcion et al., 2009) kinetically measures changes in interference patterns when the optical thickness at the tip of a biosensor coated with one type of molecule changes as a result of binding of an interacting other molecule (analyte) from the soluble phase. Here an Octet Red96 System (Pall ForteBio) system was used; amine-reactive sensors were coated with 5 μg/ml CHO cell-expressed S protein in sodium acetate buffer at pH 5.0 as recommended by the manufacturer, then set to bind various concentrations of G12-scFv or IgG12 at 37°C for 900 s, and dissociate in PBS for another 300 s. Equilibrium dissociation constant (Kd) was obtained with the Octet QK software package.

2.9 Immunofluorescence microscopy

Cells grown on collagen-coated coverslips were fixed with 4% para-formaldehyde and permeabilized with 0.25% Triton X-100. After blocking with 3% bovine serum albumin (BSA, fraction V, Sigma) in PBS for 10 min, cells were incubated with the respective primary antibodies followed by Alexa Fluor 488 or Cy3 conjugated secondary antibodies. Nuclear DNA was stained with 4', 6-diamidino-2-phenylindole (Sigma). Cells were visualized by a laser confocal scanning microscope (Leica TCS SP8). Image processing was conducted by Las AF Lite 2.6 software (Leica). Semi-quantitation of fluorescence density and co-localization analysis was done by ImageJ software. Co-localization was evaluated by Manders' overlap coefficient (MOC) ranging from 0 (for no co-localization) to 1 (for complete co-localization) (Manders et al., 1993).

2.10 Statistical analysis

Results obtained from more than three independent experiments were shown as mean values ± standard deviations. Origin 8.0 software was used to evaluate statistical significance of differences between two experimental groups and calculate 50% inhibitory concentrations (IC_{50}) in molar concentration. Statistical significance of differences between two treatment groups was assessed by one-way analysis of variance (ANOVA) using Origin 8.0.

3. Results

3.1 Soluble expression of G12-scFv in *E. coli* SHuffle T7 but not BL21 Star cells

Intra-chain disulfide bonds in the VL and VH domain of scFv are critical for correct protein folding (Liu and May, 2012), hence expression in the reducing cytoplasm of commonly used *E. coli* strains like BL21 and its derivatives often results in non-functional aggregates. Some biologically active single-domain antibodies and even IgG molecules have recently been obtained by soluble expression in the oxidative cytoplasm of *E. coli* SHuffle strain (Robinson et al., 2015; Zarschler et al., 2013), which is defective in both thioredoxin (trxB) and glutathione (gor) pathways and constitutively expresses the disulfide-bond isomerase DsbC in the cytoplasm (Lobstein et al., 2012). To test for potential benefits of using this strain we transformed SHuffle T7 and BL21 Star cells in parallel with the pET vector encoding G12-scFv with an N terminal His6-tag and C terminal HA-tag. G12-scFv expression was induced by 0.5 mM IPTG and shaking cultivation at 30°C for 16 h. SDS-PAGE comparison of small aliquots of cells from induced vs. noninduced cultures directly lysed in SDS sample buffer showed a strong new band at the expected position of ~30 kDa in both strains (Fig. 1A, lanes +/- IPTG). This was confirmed for the preparative lysates obtained by sonication-based lysis (lanes “total”). However, after the lysates were cleared by centrifugation the respective band was prominently visible only in the soluble fraction from the SHuffle T7 cells (lanes “soluble”). Hence the SHuffle T7 strain proved clearly superior over BL21 Star for soluble expression of G12-scFv.

To obtain scFvs for experimental controls, we designed analogous expression vectors for His6- plus HA-tagged scFvs derived from the HBV PreS1-specific mAb 18/7

(Glebe et al., 2003) and the HIV-1 gp120-specific mAb VRC01-IgG (Wu et al., 2010). Next we expressed all three scFvs in 600 ml SHuffle T7 cell cultures and purified them by Ni^{2+} IMAC. As expected the respective products eluted at the higher imidazole concentrations (Fig. 1B), although in substantially different amounts. Nonetheless, the pooled peak fractions from all three preparations could be sufficiently concentrated by ultrafiltration to assess protein-chemical purity by SDS-PAGE and Coomassie-Blue staining and verify the identity of ~30 kDa products by anti-His immunoblotting (Fig. 1C). The total yields per 600 ml culture for the G12-, VRC01- and 18/7-scFvs were 1.3 mg, 0.4 mg, and 0.07 mg, respectively. Hence the expression host as well as the specific sequence of a scFv contribute importantly to solubility. In addition, we also purified a mutated G12-scFv (G12-scFv-HCdel) with deletion of 11 amino acids at the CDR3 of VH (Fig. 1C).

3.2 Characterization of G12-scFv binding to S protein

The binding affinity of G12-scFv was qualitatively and quantitatively assessed by a panel of assays. First, a dilution series of CHO cell-derived S protein was subjected to NAGE where SVPs migrate as a compact band with distinctly lower mobility than nonenveloped capsids (Birnbaum and Nassal, 1990; Sun and Nassal, 2006). After capillary transfer to a nylon membrane the blots were probed with G12-scFv-HA, a commercial polyclonal anti-S as positive control, and VRC01-scFv-HA as negative control. As shown in Fig. 2A, 0.8 μg/ml G12-scFv-HA recognized the native SVPs as efficiently as 0.25 μg/ml polyclonal anti-S, with a detection limit of ~10 ng, while

VRC01-scFv-HA gave no signal at all. Consistent with the well-known importance of CDR3 of VH for antigen binding (Davies and Cohen, 1996), G12-scFv-HCdel with a deletion of 11 CDR3 residues showed nearly no more SVP binding (Fig. S1A). In addition, immunofluorescence microscopy showed G12-scFv to recognize intracellular HBs protein rather than other cellular proteins in Huh-7 cells that were transiently transfected with an HBV expression vector (Fig. 2B and Fig. S11), corroborating specificity of the HBs interaction. However, like the parental G12 mAb, G12-scFv did not react with SDS-denatured HBs protein on Western blots (data not shown). HBsAg binding specificity was further checked using two samples of pooled sera from healthy donors and CHB patients, which were confirmed to be HBsAg negative and positive, respectively, by a commercial KHB ELISA kit (Fig. 2C). Next the wells of a microtiter plate were coated with 5 μg/ml of G12-scFv, IgG12, VRC01-scFv, or skim milk; in ELISA both G12-scFv and IgG12 clearly recognized the HBsAg-positive but not the healthy donor sample, indicating specificity for HBsAg rather than other serum proteins (Fig. 2C). Besides, serum HBsAg binding affinity of G12-scFv was weaker than that of IgG12 (Fig. 2C).

To quantitatively compare the binding affinities for native S of G12-scFv versus IgG12, biolayer interferometry (Concepcion et al., 2009) was used to determine the equilibrium dissociation constants (Fig. 2D). IgG12 displayed subnanomolar binding ($Kd=5.98\times10^{-10}$ M); this is ~8-fold lower than measured by surface plasmon resonance (Wang et al., 2016), likely due to the disparate assay platforms and/or experimental

conditions. For G12-scFv, interferometry yielded a Kd value of 1.09×10^{-8} M. Though ~20-fold weaker relative to IgG12 this still represents a very high binding affinity, in particular for an scFv. Specific but weaker binding to S protein than by IgG12 was confirmed in a microtiter plate format measuring the capacities of immobilized G12-scFv vs. IgG12 to bind soluble S protein (Fig. 2E). Lastly, we assessed the ability of G12-scFv and, as an irrelevant control, of the anti-HIV gp120 VRC01-scFv to compete with S binding to immobilized IgG12 (Fig. 2F). About 1 μg of G12-scFv per well reduced the ELISA signal to 50% whereas no clear inhibition was seen with up to 20 μg of the irrelevant scFv. Hence despite lower affinity, G12-scFv bound competitively to S, in line with sharing a common conformational epitope with IgG12. The relatively high levels of G12-scFv required for competition likely relate to its lower affinity for the target antigen but also to the multiple repetitive epitopes on native SVPs which must all be blocked to prevent binding to the immobilized IgG12.

3.3 G12-scFv potently neutralized HBV infection of HepG2-NTCP cells

The parental IgG12 mAb blocked HBV infection in cultured cells with 1,000-fold higher efficiency than HBIG (Wang et al., 2016). To test the HBV neutralizing capacity of G12-scFv we first established a HepG2 cell line (HepG2-N1) which stably expresses NTCP (Fig. S2A) and is highly permissive for HBV infection (Fig. S2B-S2E). Its suitability for evaluating antiviral effects was verified by efficient post-infection inhibition of HBV replication by IFN-α and 3TC (Fig. S2D-S2E). To assess neutralization potency and specificity we preincubated HBV for 5 min with

serially diluted G12-scFv, or IgG12, or PreS1-targeting MA18/7-scFv, or the irrelevant VRC01-scFv. Next we inoculated HepG2-N1 cells overnight with the treated virus stocks at a constant nominal multiplicity of infection (MOI) of 500 viral genome equivalents (vge) per cell. Impacts on infection were monitored by HBeAg ELISA of the culture supernatants on day 5 post inoculation (Fig. 3A). G12-scFv potently blocked HBV infection, with an IC_{50} of 1.8 nM. The neutralizing activity of the parental mAb IgG12 was ~3-fold higher (IC_{50}=0.57 nM), while that of MA18/7-scFv was ~7-fold weaker (Fig. 3A). Importantly, up to 5 μg/ml of the control VRC01-scFv had no effect (Fig. 3A). In addition, Northern blotting of viral RNAs extracted at day 5 post inoculation further demonstrated dose-dependent neutralization of HBV infection by G12-scFv as well as MA18/7-scFv (Fig. 3B).

3.4 G12-scFv was internalized by hepatoma cells and PHHs

Many scFvs have been reported to be able to penetrate into tissues and cells (Ha et al., 2014; Monnier et al., 2013; Park et al., 2017; Rudnick and Adams, 2009; Safdari et al., 2016). For subsequent studies on a potential intracellular antiviral activity of G12-scFv, we first investigated internalization of G12-scFv and VRC01-scFv in the stably HBV producing hepatoma cell line 2.2.15 by LCM. Cells were incubated with 5 μg/ml of the respective scFv for 24 h, extensively washed to remove unbound scFvs, then analyzed by anti-HA immunofluorescence. Compared to the blank control (Fig. S3), both scFvs appeared to be associated with the cellular periphery and also be situated inside cells (Fig. 4A and 4B). Both scFvs co-localized with Rab5 (Fig. 4A) and Rab7

(Fig. 4B), markers of early and late endosomes in the endocytic pathway, when assessed by the MOC (Fig. 4A and 4B). G12-scFvs binding to and penetration into the 2.2.15 cells had a kinetic component in that the intracellular signals increased from 2 h over 5 h to 24 h post-incubation (Fig. S4). In addition, LCM also revealed internalization of Alexa Fluor 488 conjugated G12-scFv (A488-G12-scFv, Fig. S5A) into 2.2.15 cells and co-localization with Rab5 and Rab7 after incubation with 2.2.15 cells for 24 h (Fig. S5B). Furthermore, time lapse live-cell confocal microscopy showed that internalized A488-G12-scFv gradually decayed within 6 h after the exogenously added A488-G12-scFv was withdrawn from the culture medium (Fig. S5C), in line with intracellular degradation. Notably, in PHHs scFv uptake was also seen whereas cell surface binding was much less apparent (Fig. S6). S-independent G12-scFv internalization was further observed in naïve HepG2 cells, where endocytosed G12-scFv co-localized with Rab7 (Fig. S7 and top panels of Fig. 5A). Furthermore, nystatin and dynasore, specific small molecule inhibitors of caveolin- and dynamin-mediated cellular endocytosis (Dutta and Donaldson, 2012), significantly decreased internalization of G12-scFv into HepG2 cells (Fig. 5A and 5B), suggesting that both endocytic pathways are involved in the uptake. Collectively, these experiments indicated that G12-scFv was endocytosed by hepatoma cells via host endocytic pathways and suggested subsequent transportation into the early and late endosomes.

3.5 G12-scFv markedly suppressed virion secretion in 2.2.15 cells

To test whether G12-scFv treatment could interfere with HBV DNA replication and virion secretion, 2.2.15 cells were maintained in medium containing 5 μg/ml of G12-scFv or, as control, VRC01-scFv. Every other day, media were collected and replaced by fresh scFv-containing media until day 6 (Fig. 6A). On day 8, cells were extensively washed and treated by trypsin to remove unattached scFvs, then lysed with NP-40 lysis buffer for analysis of intracellular viral DNA and proteins. Anti-HA immunoblotting detected both scFvs in the cytoplasmic extracts (Fig. 6B), supporting the immunofluorescence-based evidence for scFv internalization by 2.2.15 cells (Fig. 4 and Fig. S5). Intracellular L protein, capsids, and capsid-borne viral DNA detected by Western blotting, NAGE, and Southern blotting, respectively, did not differ between G12- and VRC01-scFv treated cells (Fig. 6B and 6C). On the other hand, intracellular S seemed to slightly accumulate in the G12-scFv treated cells (Fig. 6B). No overt cytotoxic effects were observed for either scFv, as corroborated by cell counting kit-8 (CCK8) cell viability assays for up to 200 μg/ml of G12-scFv (Fig. S9).

To examine the impact of G12-scFv vs. the control VRC01-scFv on extracellular viral particles, virions, SVPs, and naked capsids were enriched from the pooled culture supernatants (Fig. 6A) by PEG precipitation. In NAGE, enveloped genome-free as well as genome-filled capsids comigrate with SVPs and thus can be separated from the faster migrating naked capsids (Birnbaum and Nassal, 1990; Ning et al., 2017; Sun and Nassal, 2006). Immunoblotting with a polyclonal anti-core antiserum revealed an excess of virion-associated capsids over naked capsids, regardless of the scFv (Fig.

6D). However, in the G12-scFv treated samples enveloped but not naked capsids were reduced by >50% compared to the control (Fig. 6D, top). A similar reduction was seen for extracellular virion borne DNA, which was extracted from enveloped genome-filled capsids following anti-PreS1 immunoprecipitation of PEG-precipitated extracellular viral particles (Fig. 6D, bottom). In contrast, the S binding-inactive mutant G12-scFv-HCdel did not alter extracellular virion-associated capsids (Fig. S1B). Moreover, immunoblotting of the PEG precipitates revealed a strong decrease of extracellular L protein in the G12-scFv treated samples to ~30% of that in the VRC01-scFv control (Fig. 6E). By contrast, S protein was only mildly suppressed to 70% of the control (Fig. 6E), as corroborated by an only minor reduction in the ELISA value of secreted HBsAg (Fig. 6E). Secreted HBeAg was not at all altered by G12-scFv treatment (Fig. 6E). Together, these data were in line with an S-specific effect of G12-scFv, however with a greater negative impact on both genome-free and genome-filled virions than on SVPs.

To further characterize this anti-virion effect we incubated the 2.2.15 cells with serial five-fold dilutions of G12-scFv and the control scFv, starting with 0.5 µg/ml (16.4 nM) as highest concentration. We then monitored the levels of intracellular vs. extracellular capsids (by NAGE), S protein (by Western blot) and viral DNA (by qPCR and Southern blotting). As shown in Fig. 6F and Fig. S10 (upper panels), neither G12-scFv nor the control scFv had a detectable effect on the intracellular HBV markers. However, for the extracellular samples (lower panels in Fig. 6F and Fig. S10) a

two-fold decrease in L protein and a massive (~10-fold) drop in virion-associated capsids as well as virion DNA were seen at the two highest doses of G12-scFv (IC_{50} = 1.25 nM) whereas Western blot detectable S protein remained largely unaffected. The irrelevant scFv had again only minor, if any, impacts. Increasing the scFv concentrations to 1, 2, and 5 µg/ml did not change these patterns (Fig. S8), indicating that inhibition of virion release was already maximal at 0.1 µg/ml (3.28 nM). At even higher scFv concentrations (5 to 50 µg/ml) G12-scFv, but not the control scFv, was able to reduce also extracellular S besides L while both intracellular S and L still remained unaffected (Fig. 6G). Cytotoxic effects were not responsible for the reduction in secreted virions at low and/or of S protein at high concentrations of G12-scFv as up to 200 µg/ml of the scFv did not affect cell viability (Fig. S9).

3.6 G12-scFv treatment drastically inhibited virion secretion in Huh-7 cells

To confirm that the anti-virion effects of G12-scFv were not restricted to 2.2.15 cells we monitored its impact on virion secretion from another hepatoma cell line, Huh-7, upon transfection with the HBV expressing plasmid pCH-9/3091 (Nassal, 1992). Treatment with 5 µg/ml of G12- or VRC01-scFv had no detectable influence on intracellular viral replication markers including capsids, capsid-borne viral DNA (Fig. 7A), L or S protein (Fig. 7B). However, as for 2.2.15 cells, G12-scFv treatment strongly reduced extracellular virion-associated capsid and virion DNA to ~30% of the control scFv, without affecting extracellular naked capsids (Fig. 7C). Therefore the overall reduction in extracellular HBV core proteins detected by Western blotting (Fig.

7D, middle panel) originated mostly from the loss of enveloped capsids. Extracellular L protein was also reduced to a lower level relative to the control than S protein (28.6% vs 59.7%, Fig. 7D, upper panel). Overall extracellular HBsAg levels were reduced to ~55% of the control (Fig. 7D, bottom panel). Hence G12-scFv exerted comparable anti-virion effects in two different human hepatoma cell lines.

4. Discussion

ScFvs represent a new class of promising biopharmaceuticals for diagnostic and therapeutic medicine, as evidenced by the increasing number of preclinical and clinical trials (Elgundi et al., 2017; Nelson, 2010). However, the advantages of their simplified structure may be offset by reduced target binding and lower neutralization potency. In this study, we achieved efficient production of a scFv derivative of the S protein binding, virus neutralizing mAb IgG12 in a robust, cost-effective *E. coli* expression system. Importantly, G12-scFv solubly expressed in the bacterial cytoplasm exerted target-specific high-affinity binding to S protein (Kd=10.9 nM) and inhibited HBV infection of a susceptible HepG2 cell line with only three-fold lower potency (IC_{50}=1.8 nM) than the parental mAb. Remarkably, similarly low concentrations of G12-scFv (IC_{50}=1.25 nM) interfered selectively with virion rather than SVP secretion from 2.2.15 as well as Huh-7 human hepatoma cells. This interference correlated with G12-scFv's target specificity and presumably also cellular internalization.

4.1 G12-scFv target specificity and affinity

S protein binding activity of the bacterially expressed G12-scFv was validated by a panel of assays, including NAGE of SVPs, immunofluorescence microscopy, biolayer interferometry, and ELISA (Fig. 2), all of which were in line with correct folding and disulfide bond formation. Specificity of G12-scFv for S protein was confirmed by the selective recognition, in the presence of many other proteins, of cells expressing HBsAg (Fig. 2B and Fig. S11) and of CHB patient serum (Fig. 2C). As suggested by competitive ELISA, G12-scFv bound to a conformational HBs epitope shared with that of the parental mAb IgG12 (Fig. 2F), though with ~20-fold lower affinity (Kd=10.9 nM; Fig. 2D). This is expected because in contrast to the two paratopes per IgG the scFv is monovalent, and the artificial joining of VL and VH might affect the relative orientation of the two domains and thus slightly reshape the antigen binding site (Sela-Culang et al., 2013); also, potentially beneficial allosteric impacts from the constant regions cannot occur (Sela-Culang et al., 2013). However, compared to a commercial polyclonal anti-S antiserum (Fig. 2A) and published anti-S mAbs or scFvs G12-scFv maintained an unusually high target affinity (Kim and Park, 2002; Maeda et al., 1999; Shin et al., 2007; Tajiri et al., 2010). If desired, this might be further enhanced by modern antibody engineering techniques (Saeed et al., 2017).

4.2 G12-scFv HBV neutralizing activity

Using secreted HBeAg and viral RNAs as infection markers, G12-scFv was shown to potently neutralize HBV infection (IC_{50}=1.8 nM). In view of the ~20-fold lower target affinity compared to IgG12 (Fig. 2D) a ~3-fold lower neutralizing potency may appear

surprising (Fig. 3A). However, a previous study also found no linear correlation between the antigen binding affinities and neutralization activities of antibodies targeting the “a” determinant in HBsAg (Tajiri et al., 2010). The simplest scenario for virus neutralization by such antibodies, including G12-scFv, is masking of the AGL on the virion surface, preventing its attachment to the low-affinity receptor heparan sulfate proteoglycan (Sureau and Salisse, 2013; Verrier et al., 2016). However, this mechanism should be competed by SVPs which also contain the AGL and can outnumber virions by orders of magnitude. It might therefore be considered that the structure and/or accessibility of the AGL epitopes is not strictly identical on virions versus SVPs and that some antibodies, possibly including IgG12 and G12-scFv, gain their high neutralizing potency from preferential binding to virions. One approach to verify this hypothesis would be to immunoprecipitate SVPs and virions from culture supernatants of HBV producing cells or CHB patient sera with IgG12 and G12-scFv and then compare the viral envelope proteins as well as virion-borne DNA between input and precipitated samples.

4.3 G12-scFv cell internalization and selective blocking of virion secretion

In the current study, G12-scFv was found to bind to and penetrate into hepatoma cells and PHHs (Fig. 4, Fig. 5, and Fig. S4-S7) in an S-independent manner, providing a potential link to the observed inhibition of virion secretion. To our knowledge, this is the first report on selective and potent inhibition of virion secretion by a scFv targeting S protein at a nanomolar concentration. Two previous reports have shown that intact

mAbs against S at ≥100 μg/ml (~667 nM) concentration reduced extracellular viral DNA and HBsAg (Neumann et al., 2010; Schilling et al., 2003). As extracellular viral DNA was derived from both naked nucleocapsids and virions, the mAbs' exact impact on the different extracellular particles remained unclear (Neumann et al., 2010; Schilling et al., 2003). In our study, by using NAGE to separate naked capsids from SVPs and genome-free and genome-filled virions we clearly showed that G12-scFv did not affect naked nucleocapsid secretion (upper panels of Fig. 6D and 7C, lower panel of Fig. 6F). Moreover, immunoblotting post NAGE plus qPCR as well as Southern blotting post anti-PreS1 immunoprecipitation showed that G12-scFv efficiently inhibited secretion of both genome-free and genome-filled virions at an IC_{50} of 1.25 nM (Fig. 6D, Fig. 6F, Fig. 7C, Fig. S8, and Fig. S10). Detectably decreasing HBsAg secretion required >100 fold higher concentrations of G12-scFv (Fig. 6G), attesting to a selectively virion-directed inhibition.

The ~500 fold higher anti-virion activity of G12-scFv compared to two previously reported mAbs (Neumann et al., 2010; Schilling et al., 2003) was possibly endowed by a combination of high S-binding affinity and more efficient cellular uptake. At ≥100 μg/ml concentration, uptake of the anti-S mAbs into hepatoma cells was supposedly mediated by interactions between the mAbs' IgG constant fragment (Fc) regions with cell surface Fc receptors (Neumann et al., 2010; Schilling et al., 2003). While this pathway cannot apply to the Fc-less scFvs, various other cell surface receptors may enable receptor-mediated endocytosis of scFvs and mAbs (Rudnick and Adams, 2009;

Safdari et al., 2016). HBs protein on the cell surface was not required because the nonrelated VRC01-scFv showed similar properties as G12-scFv (Fig. 4 and Fig. S6). More importantly, naïve HepG2 cells without expressing any HBV proteins still took up G12-scFv (Fig. 5 and Fig. S7). Also, immunofluorescence microscopy did not detect HBs protein on the cell surface (Fig. S11). However, a probable endocytosis-stimulating effect by low levels of cell-surface expressed HBs protein, suggested e.g. by data from anti-HBs chimeric antigen receptor (CAR) T cells (Krebs et al., 2013), is not excluded. A significant decrease of G12-scFv endocytosis by nystatin and dynasore suggested the involvement of caveolin- and dynamin-mediated endocytic pathways (Fig. 5). However, the actual mechanism of G12-scFv uptake remains to be determined.

Plausibly related to cell internalization was the efficient and selective suppression of HBV virion secretion by G12-scFv in two different hepatoma cell lines (Fig. 6 and Fig. 7). This suppression was target-specific as it was not seen with the VRC01-scFv control and G12-scFv-HCdel (Fig. S1B); also, intracellular and extracellular non-enveloped capsids and their associated DNA were not affected. Furthermore, suppression was not due to non-specific cytotoxic effects of G12-scFv (Fig. S9). Despite this selectivity, the antiviral activity of G12-scFv was particularly manifest in the extracellular samples and for virions and L but not S protein (Fig. 6 and Fig. 7), all in line with virion release as the major target for interference. Tetherin, counteracted by the HIV-1 Vpu protein, blocks the final fission of enveloped HI virions from the

cell surface (Perez-Caballero et al., 2009). However, extensive inspection by transmission electron microscopy did not reveal related surface structures on the G12-scFv treated cells (not shown). Notably, release of the L protein-rich virions and the filamentous subset of SVPs, but not the bulk of spherical SVPs which contain little L, involves the late endosome (also called MVB, (Hu and Liu, 2017). Uptake of G12-scFv via caveolin- and dynamin-mediated endocytic pathways and subsequently by an endosomal route, as suggested by its co-localization with the endosomal markers Rab5 and Rab7 (Fig. 4, Fig. 5, Fig. S5 and S7), would provide an opportunity for selective encounters with L protein and/or L-rich particles and an accompanying impairment of their secretion, perhaps by blocking interactions with host factors involved in release (Hoffmann et al., 2013; Rost et al., 2006). The selective reduction in extracellular L protein (Fig. 6 and Fig. 7) could then reflect preferential binding of G12-scFv to its target epitope as presented on L versus on S protein; alternatively, exclusion of the bulk of S protein from the MVB might already be sufficient to explain this selectivity as well as the requirement for 100-fold higher concentrations of G12-scFv to block SVP secretion.

5. Conclusions

In this study, we developed an *E. coli* derived G12-scFv with an unusually high affinity for S protein (Kd=10.9 nM). Soluble expression in the cytoplasm of *E. coli* SHuffle cells provided a convenient low-cost access to milligrams of biologically active G12-scFv, featuring highly efficient neutralizing activity (IC_{50}=1.8 nM). Most

remarkably, in a target-specific yet Fc-independent fashion G12-scFv selectively suppressed secretion of both empty and genome-filled virions, presumably correlating with its cell internalization capacity. This combination of properties should make G12-scFv a valuable new tool for HBV basic research as well as diagnostic, prophylactic and possibly therapeutic applications. Further enhancing G12-scFv′s antiviral activity by conversion into bivalent (diabodies), bispecific, or higher valency derivatives appears both feasible and highly worthwhile.

Acknowledgments

This study was in part supported by the National Natural Science Foundation of China (31370195 and 81672017 to YXW), Outstanding Young Scholar Project (C850005 to YXW) of Shanghai Municipal Health and Family Planning Commission. YXW is indebted to the Alexander von Humboldt Foundation for a revisit fellowship that allowed the short-term collaboration work at Dr. Michael Nassal's lab. TFB acknowledges funding from the European Union (ERC-AdG-2014-671231-HEPCIR and H2020-667273-HEPCAR) and the French National Research Agency LABEX ANR-10-LABX-0028_HEPSYS. SPT acknowledges a fund from Key Laboratory of Meidical Molecular Virology, Chinese Academy of Medical Sciences (2018PT31044). We are grateful to Zhenghong Yuan (Fudan University) for providing CHO cell-expressed S protein; Jiming Zhang (Huashan Hospital of Fudan University) for providing polyclonal anti-HBV core antiserum; Tianlei Ying (Fudan University) for a gift of peroxidase-conjugated polyclonal anti-Fc of IgG; Demin Yu (Ruijin Hospital,

Shanghai) for the pooled sera of CHB patients.

References

Birnbaum, F., Nassal, M., 1990. Hepatitis B virus nucleocapsid assembly: primary structure requirements in the core protein. J Virol 64, 3319-3330.

Chan, K.R., Ong, E.Z., Mok, D.Z., Ooi, E.E., 2015. Fc receptors and their influence on efficacy of therapeutic antibodies for treatment of viral diseases. Expert Rev Anti Infect Ther 13, 1351-1360.

Chen, J., Liu, Y., Zhao, J., Xu, Z., Chen, R., Si, L., Lu, S., Li, X., Wang, S., Zhang, K., Li, J., Han, J., Xu, D., 2016. Characterization of Novel Hepatitis B Virus PreS/S-Gene Mutations in a Patient with Occult Hepatitis B Virus Infection. PLoS One 11, e0155654.

Concepcion, J., Witte, K., Wartchow, C., Choo, S., Yao, D., Persson, H., Wei, J., Li, P., Heidecker, B., Ma, W., Varma, R., Zhao, L.S., Perillat, D., Carricato, G., Recknor, M., Du, K., Ho, H., Ellis, T., Gamez, J., Howes, M., Phi-Wilson, J., Lockard, S., Zuk, R., Tan, H., 2009. Label-free detection of biomolecular interactions using BioLayer interferometry for kinetic characterization. Comb Chem High Throughput Screen 12, 791-800.

Davies, D.R., Cohen, G.H., 1996. Interactions of protein antigens with antibodies. Proc Natl Acad Sci U S A 93, 7-12.

Dutta, D., Donaldson, J.G., 2012. Search for inhibitors of endocytosis: Intended specificity and unintended consequences. Cell Logist 2, 203-208.

Elgundi, Z., Reslan, M., Cruz, E., Sifniotis, V., Kayser, V., 2017. The state-of-play and future of antibody therapeutics. Adv Drug Deliv Rev 122, 2-19.

Glebe, D., Aliakbari, M., Krass, P., Knoop, E.V., Valerius, K.P., Gerlich, W.H., 2003. Pre-s1 antigen-dependent infection of Tupaia hepatocyte cultures with human hepatitis B virus. J Virol 77, 9511-9521.

Ha, K.D., Bidlingmaier, S.M., Zhang, Y., Su, Y., Liu, B., 2014. High-content analysis of antibody phage-display library selection outputs identifies tumor selective macropinocytosis-dependent rapidly internalizing antibodies. Mol Cell Proteomics 13, 3320-3331.

Heermann, K.H., Goldmann, U., Schwartz, W., Seyffarth, T., Baumgarten, H., Gerlich, W.H., 1984. Large surface proteins of hepatitis B virus containing the pre-s sequence. J Virol 52, 396-402.

Hoffmann, J., Boehm, C., Himmelsbach, K., Donnerhak, C., Roettger, H., Weiss, T.S., Ploen, D., Hildt, E., 2013. Identification of alpha-taxilin as an essential factor for the life cycle of hepatitis B virus. J Hepatol 59, 934-941.

Hu, J., Liu, K., 2017. Complete and Incomplete Hepatitis B Virus Particles: Formation, Function, and Application. Viruses 9.

Huovila, A.P., Eder, A.M., Fuller, S.D., 1992. Hepatitis B surface antigen assembles in a post-ER, pre-Golgi compartment. J Cell Biol 118, 1305-1320.

Kang, C., Xia, L., Chen, Y., Zhang, T., Wang, Y., Zhou, B., You, M., Yuan, Q., Tzeng, C.M., An, Z., Luo, W., Xia, N., 2018. A novel therapeutic anti-HBV antibody with increased binding to human FcRn improves in vivo PK in mice and monkeys. Protein Cell 9, 130-134.

Khan, N., Guarnieri, M., Ahn, S.H., Li, J., Zhou, Y., Bang, G., Kim, K.H., Wands, J.R., Tong, S., 2004. Modulation of hepatitis B virus secretion by naturally occurring mutations in the S gene. J Virol 78, 3262-3270.

Kian Chua, P., Lin, M.H., Shih, C., 2006. Potent inhibition of human Hepatitis B virus replication by a host factor Vps4. Virology 354, 1-6.

Kim, S.H., Park, S.Y., 2002. Selection and characterization of human antibodies against hepatitis B virus surface

antigen (HBsAg) by phage-display. Hybrid Hybridomics 21, 385-392.
Kluge, B., Schlager, M., Pairan, A., Bruss, V., 2005. Determination of the minimal distance between the matrix and transmembrane domains of the large hepatitis B virus envelope protein. J Virol 79, 7918-7921.
Krebs, K., Bottinger, N., Huang, L.R., Chmielewski, M., Arzberger, S., Gasteiger, G., Jager, C., Schmitt, E., Bohne, F., Aichler, M., Uckert, W., Abken, H., Heikenwalder, M., Knolle, P., Protzer, U., 2013. T cells expressing a chimeric antigen receptor that binds hepatitis B virus envelope proteins control virus replication in mice. Gastroenterology 145, 456-465.
Krieger, S.E., Zeisel, M.B., Davis, C., Thumann, C., Harris, H.J., Schnober, E.K., Mee, C., Soulier, E., Royer, C., Lambotin, M., Grunert, F., Dao Thi, V.L., Dreux, M., Cosset, F.L., McKeating, J.A., Schuster, C., Baumert, T.F., 2010. Inhibition of hepatitis C virus infection by anti-claudin-1 antibodies is mediated by neutralization of E2-CD81-claudin-1 associations. Hepatology 51, 1144-1157.
Kuttner, G., Kramer, A., Schmidtke, G., Giessmann, E., Dong, L., Roggenbuck, D., Scholz, C., Seifert, M., Stigler, R.D., Schneider-Mergener, J., Porstmann, T., Hohne, W., 1999. Characterization of neutralizing anti-pre-S1 and anti-pre-S2 (HBV) monoclonal antibodies and their fragments. Mol Immunol 36, 669-683.
Kwei, K., Tang, X., Lok, A.S., Sureau, C., Garcia, T., Li, J., Wands, J., Tong, S., 2013. Impaired virion secretion by hepatitis B virus immune escape mutants and its rescue by wild-type envelope proteins or a second-site mutation. J Virol 87, 2352-2357.
Ladner, S.K., Otto, M.J., Barker, C.S., Zaifert, K., Wang, G.H., Guo, J.T., Seeger, C., King, R.W., 1997. Inducible expression of human hepatitis B virus (HBV) in stably transfected hepatoblastoma cells: a novel system for screening potential inhibitors of HBV replication. Antimicrob Agents Chemother 41, 1715-1720.
Lambert, C., Doring, T., Prange, R., 2007. Hepatitis B virus maturation is sensitive to functional inhibition of ESCRT-III, Vps4, and gamma 2-adaptin. J Virol 81, 9050-9060.
Li, Z., Krippendorff, B.F., Sharma, S., Walz, A.C., Lave, T., Shah, D.K., 2016. Influence of molecular size on tissue distribution of antibody fragments. MAbs 8, 113-119.
Liu, H., May, K., 2012. Disulfide bond structures of IgG molecules: structural variations, chemical modifications and possible impacts to stability and biological function. MAbs 4, 17-23.
Lobstein, J., Emrich, C.A., Jeans, C., Faulkner, M., Riggs, P., Berkmen, M., 2012. SHuffle, a novel Escherichia coli protein expression strain capable of correctly folding disulfide bonded proteins in its cytoplasm. Microb Cell Fact 11, 56.
Maeda, F., Nagatsuka, Y., Ihara, S., Aotsuka, S., Ono, Y., Inoko, H., Takekoshi, M., 1999. Bacterial expression of a human recombinant monoclonal antibody fab fragment against hepatitis B surface antigen. J Med Virol 58, 338-345.
Mailly, L., Xiao, F., Lupberger, J., Wilson, G.K., Aubert, P., Duong, F.H.T., Calabrese, D., Leboeuf, C., Fofana, I., Thumann, C., Bandiera, S., Lutgehetmann, M., Volz, T., Davis, C., Harris, H.J., Mee, C.J., Girardi, E., Chane-Woon-Ming, B., Ericsson, M., Fletcher, N., Bartenschlager, R., Pessaux, P., Vercauteren, K., Meuleman, P., Villa, P., Kaderali, L., Pfeffer, S., Heim, M.H., Neunlist, M., Zeisel, M.B., Dandri, M., McKeating, J.A., Robinet, E., Baumert, T.F., 2015. Clearance of persistent hepatitis C virus infection in humanized mice using a claudin-1-targeting monoclonal antibody. Nat Biotechnol 33, 549-554.
Manders, E.M.M., Verbeek, F.J., Aten, J.A., 1993. Measurement of co-localization of objects in dual-colour confocal images. Journal of Microscopy 169, 375-382.
Mangold, C.M., Unckell, F., Werr, M., Streeck, R.E., 1995. Secretion and antigenicity of hepatitis B virus small envelope proteins lacking cysteines in the major antigenic region. Virology 211, 535-543.
Monnier, P., Vigouroux, R., Tassew, N., 2013. In Vivo Applications of Single Chain Fv (Variable Domain) (scFv) Fragments. Antibodies 2, 193-208.

Nassal, M., 1992. The arginine-rich domain of the hepatitis B virus core protein is required for pregenome encapsidation and productive viral positive-strand DNA synthesis but not for virus assembly. J Virol 66, 4107-4116.

Nelson, A.L., 2010. Antibody fragments: hope and hype. MAbs 2, 77-83.

Neumann, A.U., Phillips, S., Levine, I., Ijaz, S., Dahari, H., Eren, R., Dagan, S., Naoumov, N.V., 2010. Novel mechanism of antibodies to hepatitis B virus in blocking viral particle release from cells. Hepatology 52, 875-885.

Ni, Y., Lempp, F.A., Mehrle, S., Nkongolo, S., Kaufman, C., Falth, M., Stindt, J., Koniger, C., Nassal, M., Kubitz, R., Sultmann, H., Urban, S., 2014. Hepatitis B and D viruses exploit sodium taurocholate co-transporting polypeptide for species-specific entry into hepatocytes. Gastroenterology 146, 1070-1083.

Ning, X., Basagoudanavar, S.H., Liu, K., Luckenbaugh, L., Wei, D., Wang, C., Wei, B., Zhao, Y., Yan, T., Delaney, W., Hu, J., 2017. Capsid Phosphorylation State and Hepadnavirus Virion Secretion. J Virol 91.

Pairan, A., Bruss, V., 2009. Functional surfaces of the hepatitis B virus capsid. J Virol 83, 11616-11623.

Park, H., Kim, M., Kim, H.J., Lee, Y., Seo, Y., Pham, C.D., Lee, J., Byun, S.J., Kwon, M.H., 2017. Heparan sulfate proteoglycans (HSPGs) and chondroitin sulfate proteoglycans (CSPGs) function as endocytic receptors for an internalizing anti-nucleic acid antibody. Sci Rep 7, 14373.

Patzer, E.J., Nakamura, G.R., Yaffe, A., 1984. Intracellular transport and secretion of hepatitis B surface antigen in mammalian cells. J Virol 51, 346-353.

Perez-Caballero, D., Zang, T., Ebrahimi, A., McNatt, M.W., Gregory, D.A., Johnson, M.C., Bieniasz, P.D., 2009. Tetherin inhibits HIV-1 release by directly tethering virions to cells. Cell 139, 499-511.

Robinson, M.P., Ke, N., Lobstein, J., Peterson, C., Szkodny, A., Mansell, T.J., Tuckey, C., Riggs, P.D., Colussi, P.A., Noren, C.J., Taron, C.H., DeLisa, M.P., Berkmen, M., 2015. Efficient expression of full-length antibodies in the cytoplasm of engineered bacteria. Nat Commun 6, 8072.

Rost, M., Mann, S., Lambert, C., Doring, T., Thome, N., Prange, R., 2006. Gamma-adaptin, a novel ubiquitin-interacting adaptor, and Nedd4 ubiquitin ligase control hepatitis B virus maturation. J Biol Chem 281, 29297-29308.

Rudnick, S.I., Adams, G.P., 2009. Affinity and avidity in antibody-based tumor targeting. Cancer Biother Radiopharm 24, 155-161.

Saeed, A.F., Wang, R., Ling, S., Wang, S., 2017. Antibody Engineering for Pursuing a Healthier Future. Front Microbiol 8, 495.

Safdari, Y., Ahmadzadeh, V., Khalili, M., Jaliani, H.Z., Zarei, V., Erfani-Moghadam, V., 2016. Use of single chain antibody derivatives for targeted drug delivery. Mol Med 22, 258-270.

Salazar, G., Zhang, N., Fu, T.M., An, Z., 2017. Antibody therapies for the prevention and treatment of viral infections. NPJ Vaccines 2, 19.

Schilling, R., Ijaz, S., Davidoff, M., Lee, J.Y., Locarnini, S., Williams, R., Naoumov, N.V., 2003. Endocytosis of hepatitis B immune globulin into hepatocytes inhibits the secretion of hepatitis B virus surface antigen and virions. J Virol 77, 8882-8892.

Sela-Culang, I., Kunik, V., Ofran, Y., 2013. The structural basis of antibody-antigen recognition. Front Immunol 4, 302.

Sells, M.A., Chen, M.L., Acs, G., 1987. Production of hepatitis B virus particles in Hep G2 cells transfected with cloned hepatitis B virus DNA. Proc Natl Acad Sci U S A 84, 1005-1009.

Shin, Y.W., Ryoo, K.H., Hong, K.W., Chang, K.H., Choi, J.S., So, M., Kim, P.K., Park, J.Y., Bong, K.T., Kim, S.H., 2007. Human monoclonal antibody against Hepatitis B virus surface antigen (HBsAg). Antiviral Res 75, 113-120.

Sun, D., Nassal, M., 2006. Stable HepG2- and Huh7-based human hepatoma cell lines for efficient regulated

expression of infectious hepatitis B virus. J Hepatol 45, 636-645.
Sureau, C., Salisse, J., 2013. A conformational heparan sulfate binding site essential to infectivity overlaps with the conserved hepatitis B virus a-determinant. Hepatology 57, 985-994.
Tajiri, K., Ozawa, T., Jin, A., Tokimitsu, Y., Minemura, M., Kishi, H., Sugiyama, T., Muraguchi, A., 2010. Analysis of the epitope and neutralizing capacity of human monoclonal antibodies induced by hepatitis B vaccine. Antiviral Res 87, 40-49.
Torres, M., Casadevall, A., 2008. The immunoglobulin constant region contributes to affinity and specificity. Trends Immunol 29, 91-97.
Trepo, C., Chan, H.L., Lok, A., 2014. Hepatitis B virus infection. Lancet 384, 2053-2063.
Urban, S., Bartenschlager, R., Kubitz, R., Zoulim, F., 2014. Strategies to inhibit entry of HBV and HDV into hepatocytes. Gastroenterology 147, 48-64.
Verrier, E.R., Colpitts, C.C., Bach, C., Heydmann, L., Weiss, A., Renaud, M., Durand, S.C., Habersetzer, F., Durantel, D., Abou-Jaoude, G., Lopez Ledesma, M.M., Felmlee, D.J., Soumillon, M., Croonenborghs, T., Pochet, N., Nassal, M., Schuster, C., Brino, L., Sureau, C., Zeisel, M.B., Baumert, T.F., 2016. A targeted functional RNA interference screen uncovers glypican 5 as an entry factor for hepatitis B and D viruses. Hepatology 63, 35-48.
Wang, W., Sun, L., Li, T., Ma, Y., Li, J., Liu, Y., Li, M., Wang, L., Li, C., Xie, Y., Wen, Y., Liang, M., Chen, L., Tong, S., 2016. A human monoclonal antibody against small envelope protein of hepatitis B virus with potent neutralization effect. MAbs 8, 468-477.
Wang, Y.X., Wen, Y.M., Nassal, M., 2012. Carbonyl J acid derivatives block protein priming of hepadnaviral P protein and DNA-dependent DNA synthesis activity of hepadnaviral nucleocapsids. J Virol 86, 10079-10092.
Watanabe, T., Sorensen, E.M., Naito, A., Schott, M., Kim, S., Ahlquist, P., 2007. Involvement of host cellular multivesicular body functions in hepatitis B virus budding. Proc Natl Acad Sci U S A 104, 10205-10210.
Wounderlich, G., Bruss, V., 1996. Characterization of early hepatitis B virus surface protein oligomers. Arch Virol 141, 1191-1205.
Wu, X., Yang, Z.Y., Li, Y., Hogerkorp, C.M., Schief, W.R., Seaman, M.S., Zhou, T., Schmidt, S.D., Wu, L., Xu, L., Longo, N.S., McKee, K., O'Dell, S., Louder, M.K., Wycuff, D.L., Feng, Y., Nason, M., Doria-Rose, N., Connors, M., Kwong, P.D., Roederer, M., Wyatt, R.T., Nabel, G.J., Mascola, J.R., 2010. Rational design of envelope identifies broadly neutralizing human monoclonal antibodies to HIV-1. Science 329, 856-861.
Zanetti, A.R., Van Damme, P., Shouval, D., 2008. The global impact of vaccination against hepatitis B: a historical overview. Vaccine 26, 6266-6273.
Zarschler, K., Witecy, S., Kapplusch, F., Foerster, C., Stephan, H., 2013. High-yield production of functional soluble single-domain antibodies in the cytoplasm of Escherichia coli. Microb Cell Fact 12, 97.
Zeisel, M.B., Lucifora, J., Mason, W.S., Sureau, C., Beck, J., Levrero, M., Kann, M., Knolle, P.A., Benkirane, M., Durantel, D., Michel, M.L., Autran, B., Cosset, F.L., Strick-Marchand, H., Trepo, C., Kao, J.H., Carrat, F., Lacombe, K., Schinazi, R.F., Barre-Sinoussi, F., Delfraissy, J.F., Zoulim, F., 2015. Towards an HBV cure: state-of-the-art and unresolved questions--report of the ANRS workshop on HBV cure. Gut 64, 1314-1326.
Zhang, T.Y., Yuan, Q., Zhao, J.H., Zhang, Y.L., Yuan, L.Z., Lan, Y., Lo, Y.C., Sun, C.P., Wu, C.R., Zhang, J.F., Zhang, Y., Cao, J.L., Guo, X.R., Liu, X., Mo, X.B., Luo, W.X., Cheng, T., Chen, Y.X., Tao, M.H., Shih, J.W., Zhao, Q.J., Zhang, J., Chen, P.J., Yuan, Y.A., Xia, N.S., 2016. Prolonged suppression of HBV in mice by a novel antibody that targets a unique epitope on hepatitis B surface antigen. Gut 65, 658-671.

Figure legends

Fig. 1. Expression and purification of histidine-tagged recombinant scFvs. (A)

Soluble expression of 6×His tagged G12-scFv in SHuffle T7 but not BL21 Star cells. Total lysates and their soluble fractions from cells of the indicated *E. coli* strains with or without IPTG treatment were analyzed by SDS-12.5% PAGE and Coomassie-Blue staining (CBS). The position of the ~30 kDa His-G12-scFv-HA protein is indicated by an arrowhead. (B) Purification of 6×His tagged scFvs through Ni-NTA chromatography. G12-, VRC01-, and MA 18/7-scFv bound the Ni-NTA columns were eluted with a linear concentration gradient (96 mM-416 mM) of imidazole and analyzed by SDS-PAGE and CBS. (C) Verification of the size and purity of concentrated scFvs. SDS-PAGE followed by CBS (upper panel) and by anti-His Western blotting (lower panel) showed major bands for G12-, VRC01-, MA 18/7-scFv, and G12-scFv-HCdel at the expected positions of 30.5 KDa, 29.5 KDa, 29.1 KDa, and 28 KDa, respectively.

Fig. 2. G12-scFv binding to SVP and native S protein. (A) Detection of G12-scFv binding to SVP by NAGE and immunoblotting. SVPs from CHO cells were separated by NAGE and transferred onto a nylon membrane. The membrane was sliced into three pieces for immunoblotting using rabbit polyclonal anti-HBs, G12-scFv-HA, and VRC01-scFv-HA respectively. (B) Detection of G12-scFv binding to intracellular HBs protein by immunofluorescence microscopy. Huh-7 cells were transfected, or not, with the HBV expressing plasmid pCH-9/3091 and subjected for immunostaining with 0.5 μg/ml G12-scFv-HA, anti-HA, and Cy3-conjugated secondary antibodies. Cells were visualized by LCM. (C) Specific binding of G12-scFv and IgG12 to HBsAg in the

pooled sera of CHB patients. Pooled sera from healthy donors and CHB patients, confirmed as HBsAg negative and positive, respectively, in a commercial anti-HBs ELISA (KHB) were ten-fold diluted in PBS and incubated in the wells of a microtiter plate coated with 5 μg/ml milk, VRC01-scFv, G12-scFv, or IgG12. Pre-coated wells from the KHB kit served as control. Bound HBsAg was then detected using the kit reagents. (D) Biolayer interferometry to measure binding affinity of G12-scFv to recombinant S from CHO cells. (E) ELISA detection of G12-scFv binding to recombinant S protein. (F) Competitive S binding to IgG12 and G12-scFv.

Fig. 3. Dose-dependent inhibition of HBV infection by G12-scFv. HepG2-N1 cells were inoculated overnight with 500 vge/cell HBV which had been incubated for 5 min with serially diluted VRC01-, G12-, or MA 18/7-scFvs or with IgG12. After extensive washing, cells were cultured in DMEM containing 2.5% DMSO. Secreted HBeAg in 10-fold diluted supernatants (A), or intracellular viral RNAs (B) were detected at day 5 post-inoculation by ELISA and Northern blotting, respectively. $A_{450\ nm}$ values with subtracting the cutoff value of 0.12 for the HBeAg test were shown. IC_{50} was calculated with Origin 8.0 software. pc RNA, precore mRNA; pgRNA, pregenomic RNA. For comparison, signal intensity of pc/pgRNA was normalized to that of GAPDH mRNA (as the loading control). Normalized values from untreated cells were set at 100%.

Fig. 4. VRC01- and G12-scFvs were internalized to 2.2.15 cells and co-localized

with Rab5 and Rab7. 2.2.15 cells were treated with 5 μg/ml of scFvs for 24 h and fixed. Incubation with rat anti-HA and rabbit anti-Rab7 or anti-Rab5 primary antibodies was followed by Cy3- and Alexa Fluor 488-conjugated secondary antibodies. Signals of Rab5 or Rab7 (in green) and scFv (in red) were visualized by LCM. Images inside the squares with the dashed outlines are shown in higher magnification. MOC was measured by ImageJ software and was used to evaluate the co-localization between Rab5 or Rab7 and scFvs.

Fig. 5. Significant inhibition of G12-scFv internalization into HepG2 cells by nystatin and dynasore. HepG2 cells grown on collagen coated coverslips were pretreated with DMSO, 50 μg/ml nystatin, and 40 μM dynasore at 37 °C for 1 h, and were then supplemented with 10 μg/ml G12-scFv for 6 h. Cells were extensively washed and immunofluorescently stained by antibodies against Rab7 and HA tag. (A) Representative LCM images showing G12-scFv internalization and co-localization between G12-scFv and Rab7. (B) Nystatin and dynasore significantly inhibited G12-scFv internalization. More than 20 randomly-picked visual fields with similar cell counts from each treatment group were captured and were semi-quantitated by ImageJ software for fluorescence densities of G12-scFvs. Significance of difference between vehicle and compound treatment groups was deduced by ANOVA and box plot analysis using Origin 8.0 software. The average fluorescence densities were labeled with orange bars.

Fig. 6. G12-scFv dose-dependently suppressed HBV virion secretion from 2.2.15 cells. (A) Experimental procedure. Five million 2.2.15 cells per well were seeded into six-well plates and were cultured in DMEM supplemented with VRC01-scFv or G12-scFv, with medium changes every second day. Two ml culture supernatant from each well was collected every two days from day 4 to day 8 post-treatment with scFv. Cells were harvested at day 8 post-treatment. Intra, intracellular samples; Extra, extracellular samples; v. capsid, virion-associated capsids; n. capsids, naked capsids. Blotting signals were semi-quantitated by MultiGauge V2.2 software. For comparison, detection signals of VRC01-scFv treatment group or non-treatment group were set at 100%. (B) Western blotting analysis of intracellular proteins. (C) Analysis of intracellular capsid and capsid-associated HBV DNA by NAGE and Southern blotting. (D) Determination of extracellular virion associated capsids (v. capsid) and naked capsids (n. capsid) by NAGE and virion borne DNA by qPCR. Short- and long-time exposures of the same blot are shown to better visualize the naked capsids. (E) Analysis of extracellular proteins by Western blotting and detection of secreted HBs and HBe antigens by ELISA. (F) G12-scFv suppressed virion secretion selectively and dose-dependently. (G) Dose-dependent inhibition of HBsAg secretion by G12-scFv. *, non-specific band, which only occurred when using a commercial polyclonal anti-S antibody from Abcam.

Fig. 7. G12-scFv potently suppressed virion secretion from Huh-7 cells. Four million Huh-7 cells per well grown in six-well plates were transfected with

pCH-9/3091 plasmid, and cultured in DMEM supplemented with 5 μg/ml of VRC01-scFv or G12-scFv. Culture supernatants were collected according to the procedure in Fig. 6A. Blotting signals were semi-quantitated by MultiGauge V2.2 software. For comparison, signals of VRC01-scFv treatment group were set at 100%. Intra, intracellular samples; Extra, extracellular samples. (A) Analysis of intracellular capsids and capsid-associated HBV DNA by NAGE and Southern blotting. (B) Western blotting analysis of intracellular proteins. (C) Determination of extracellular virion-associated capsids and naked capsids by NAGE and virion DNA by qPCR. (D) Analysis of extracellular proteins by Western blotting and detection of secreted HBs antigen by ELISA.

Fig. 1

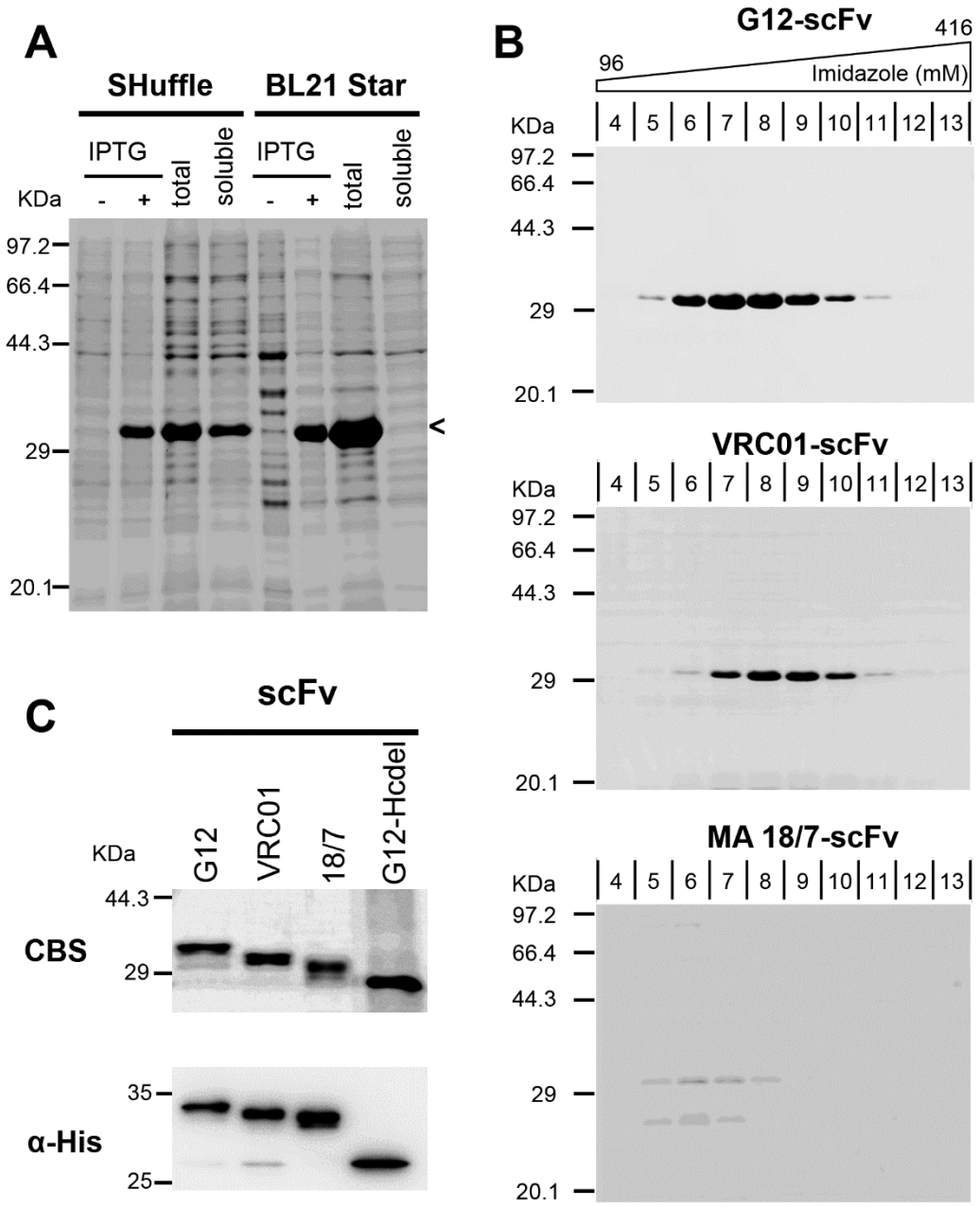
A
SHuffle
BL21 Star
IPTG
total
soluble
KDa
97.2
66.4
44.3
29
20.1
B
G12-scFv
96
416
Imidazole (mM)
4 5 6 7 8 9 10 11 12 13
VRC01-scFv
MA 18/7-scFv
C
scFv
G12
VRC01
18/7
G12-Hcdel
CBS
α-His
35
25

Fig. 2

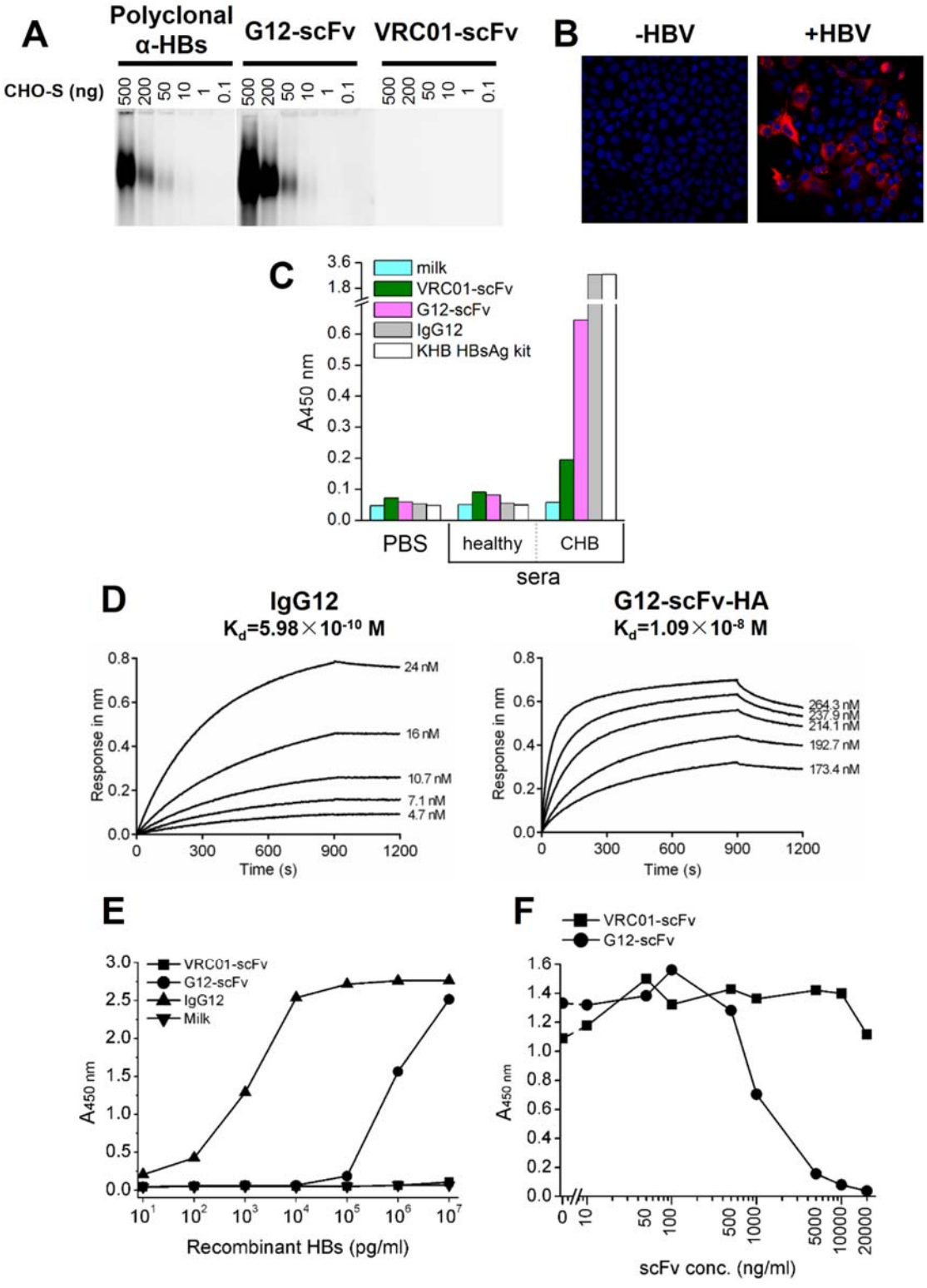
A
Polyclonal α-HBs
G12-scFv
VRC01-scFv
CHO-S (ng)
500 200 50 10 1 0.1
B
-HBV
+HBV
C
milk
VRC01-scFv
G12-scFv
IgG12
KHB HBsAg kit
A450 nm
PBS
healthy
CHB
sera
D
IgG12
Kd=5.98×10-10 M
G12-scFv-HA
Kd=1.09×10-8 M
Response in nm
Time (s)
24 nM
16 nM
10.7 nM
7.1 nM
4.7 nM
264.3 nM
237.9 nM
214.1 nM
192.7 nM
173.4 nM
E
VRC01-scFv
G12-scFv
IgG12
Milk
A450 nm
Recombinant HBs (pg/ml)
F
VRC01-scFv
G12-scFv
A450 nm
scFv conc. (ng/ml)

Fig. 3

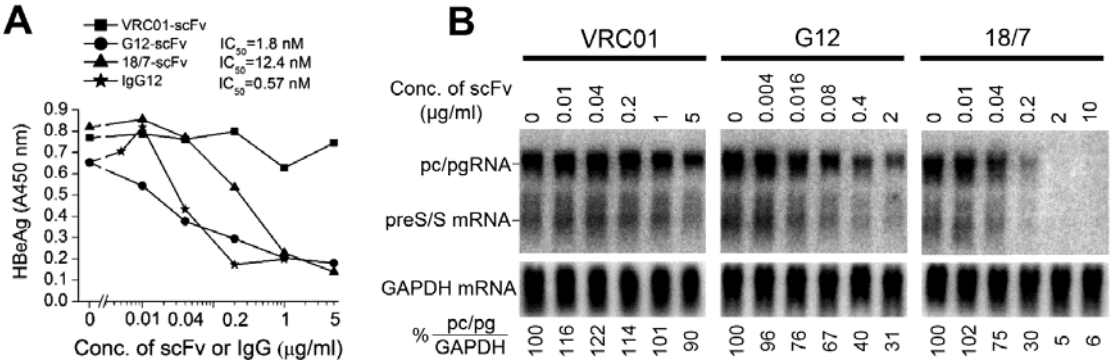
A
VRC01-scFv
G12-scFv
18/7-scFv
IgG12
IC50=1.8 nM
IC50=12.4 nM
IC50=0.57 nM
HBeAg (A450 nm)
0.9
0.8
0.7
0.6
0.5
0.4
0.3
0.2
0.1
0.0
0
0.01
0.04
0.2
1
5
Conc. of scFv or IgG (μg/ml)
B
VRC01
G12
18/7
Conc. of scFv (μg/ml)
0
0.01
0.04
0.2
1
5
0
0.004
0.016
0.08
0.4
2
0
0.01
0.04
0.2
2
10
pc/pgRNA
preS/S mRNA
GAPDH mRNA
% pc/pg / GAPDH
100
116
122
114
101
90
100
96
76
67
40
31
100
102
75
30
5
6

Fig. 4

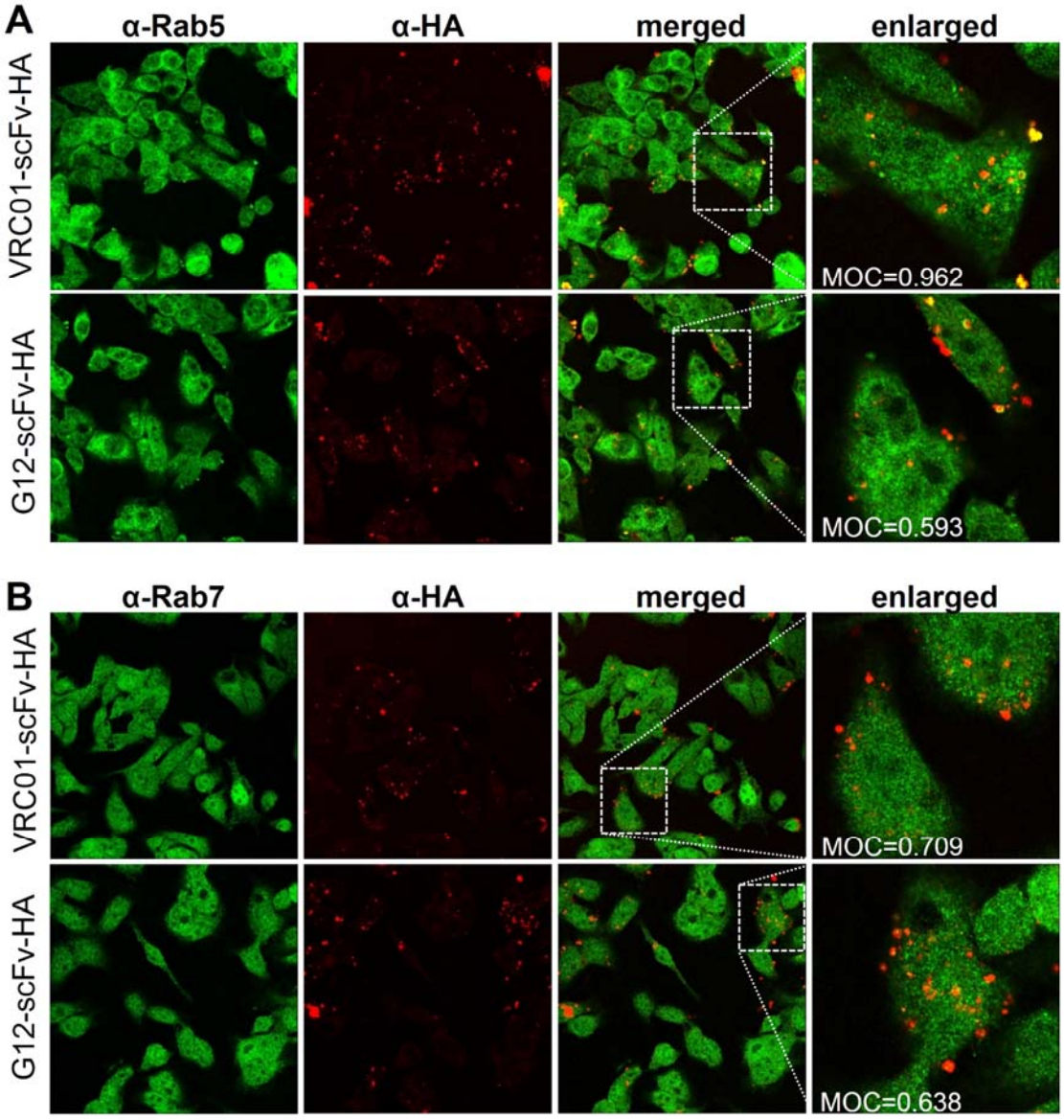
A
α-Rab5
α-HA
merged
enlarged
VRC01-scFv-HA
G12-scFv-HA
MOC=0.962
MOC=0.593
B
α-Rab7
α-HA
merged
enlarged
VRC01-scFv-HA
G12-scFv-HA
MOC=0.709
MOC=0.638

Fig. 5

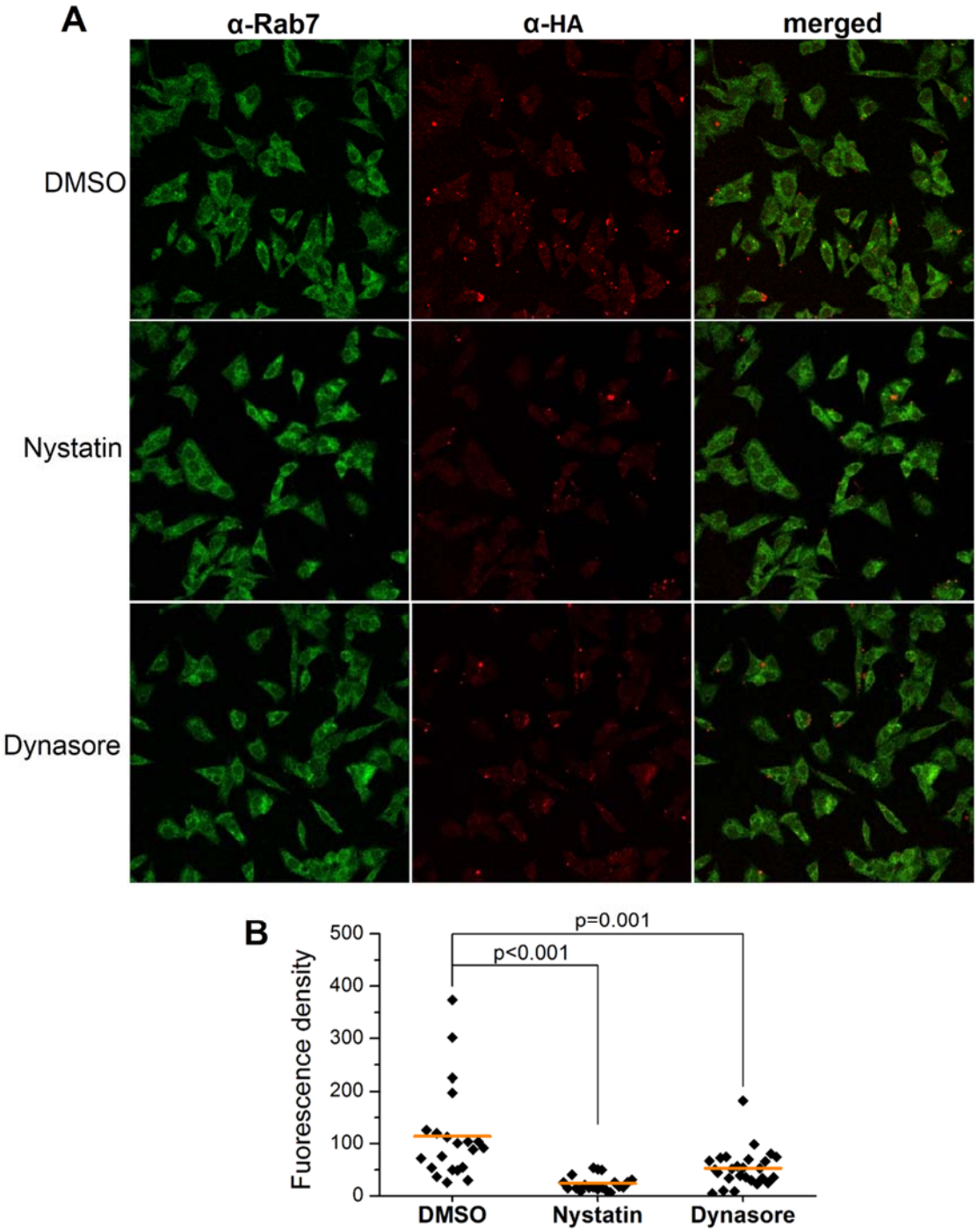
A
α-Rab7
α-HA
merged
DMSO
Nystatin
Dynasore
B
Fuorescence density
500
400
300
200
100
0
p=0.001
p<0.001
DMSO
Nystatin
Dynasore

Fig. 6

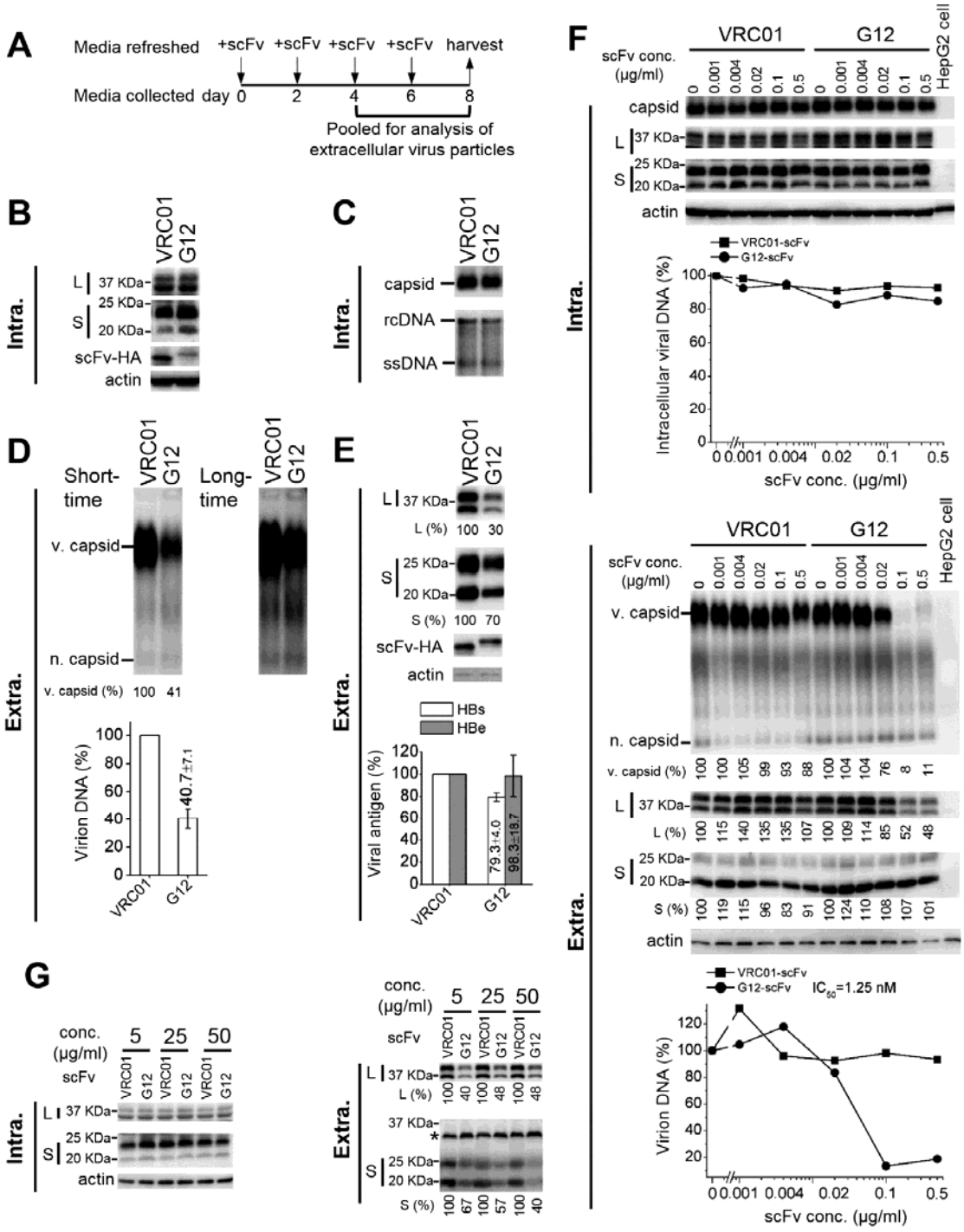
A
Media refreshed
+scFv +scFv +scFv +scFv harvest
Media collected day 0 2 4 6 8
Pooled for analysis of extracellular virus particles
B
Intra.
VRC01 G12
L 37 KDa
S 25 KDa
20 KDa
scFv-HA
actin
C
Intra.
VRC01 G12
capsid
rcDNA
ssDNA
D
Extra.
Short-time
Long-time
VRC01 G12
v. capsid
n. capsid
v. capsid (%) 100 41
Virion DNA (%)
40.7±7.1
VRC01 G12
E
Extra.
VRC01 G12
L 37 KDa
L (%) 100 30
S 25 KDa
20 KDa
S (%) 100 70
scFv-HA
actin
HBs
HBe
Viral antigen (%)
79.3±4.0
98.3±18.7
VRC01 G12
F
Intra.
VRC01 G12
scFv conc. (μg/ml)
0 0.001 0.004 0.02 0.1 0.5 0 0.001 0.004 0.02 0.1 0.5
HepG2 cell
capsid
L 37 KDa
S 25 KDa
20 KDa
actin
VRC01-scFv
G12-scFv
Intracellular viral DNA (%)
scFv conc. (μg/ml)
Extra.
VRC01 G12
scFv conc. (μg/ml)
0 0.001 0.004 0.02 0.1 0.5 0 0.001 0.004 0.02 0.1 0.5
HepG2 cell
v. capsid
n. capsid
v. capsid (%) 100 100 105 99 93 88 100 104 104 76 8 11
L 37 KDa
L (%) 100 115 140 135 135 107 100 109 114 85 52 48
S 25 KDa
20 KDa
S (%) 100 119 115 96 83 91 100 124 110 108 107 101
actin
VRC01-scFv
G12-scFv
IC50=1.25 nM
Virion DNA (%)
scFv conc. (μg/ml)
G
Intra.
conc. (μg/ml) 5 25 50
scFv VRC01 G12 VRC01 G12 VRC01 G12
L 37 KDa
S 25 KDa
20 KDa
actin
Extra.
conc. (μg/ml) 5 25 50
scFv VRC01 G12 VRC01 G12 VRC01 G12
L 37 KDa
L (%) 100 40 100 48 100 48
37 KDa
*
S 25 KDa
20 KDa
S (%) 100 67 100 57 100 40

Fig. 7

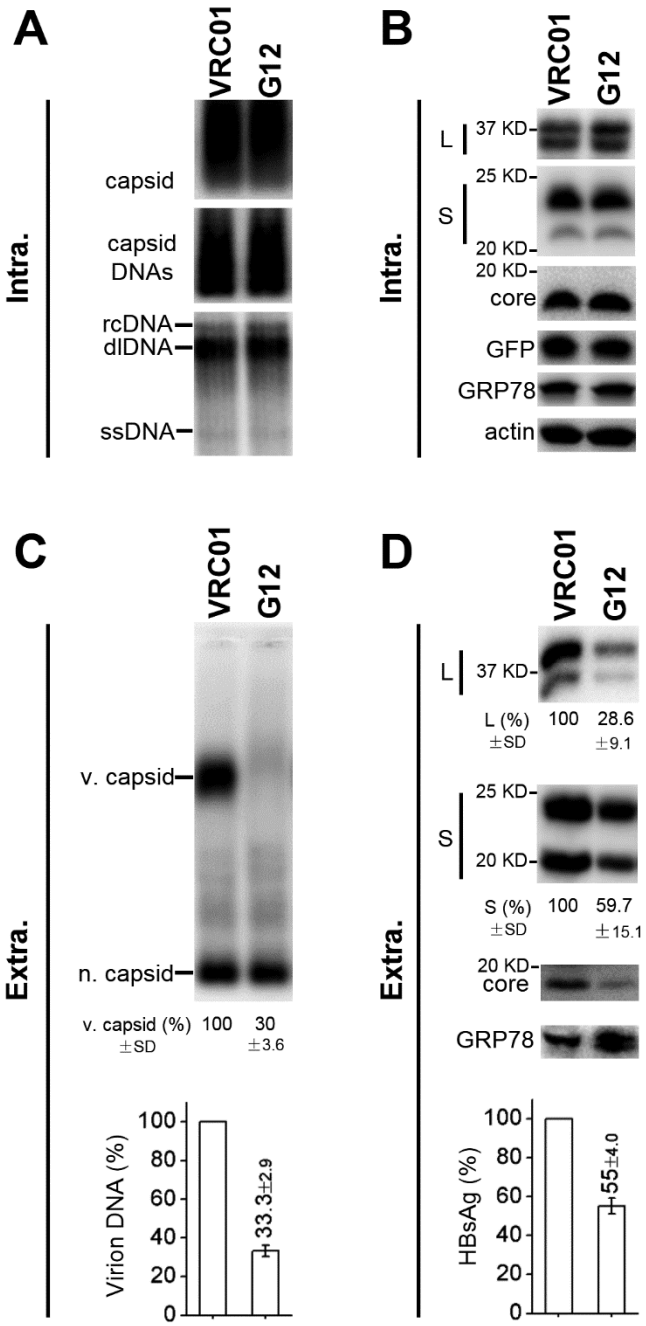
A
VRC01
G12
Intra.
capsid
capsid
DNAs
rcDNA
dlDNA
ssDNA
B
VRC01
G12
Intra.
L
37 KD
S
25 KD
20 KD
20 KD
core
GFP
GRP78
actin
C
VRC01
G12
Extra.
v. capsid
n. capsid
v. capsid (%) 100 30
±SD ±3.6
Virion DNA (%)
100
80
60
40
20
0
33.3±2.9
D
VRC01
G12
Extra.
L
37 KD
L (%) 100 28.6
±SD ±9.1
S
25 KD
20 KD
S (%) 100 59.7
±SD ±15.1
20 KD
core
GRP78
HBsAg (%)
100
80
60
40
20
0
55±4.0